Journal of Neuro-Oncology (2022) 157:49–61
https://doi.org/10.1007/s11060-021-03935-z

CLINICAL STUDY

Eigenvector PageRank difference as a measure to reveal topological characteristics of the brain connectome for neurosurgery

Onur Tanglay[1,2] · Isabella M. Young[1] · Nicholas B. Dadario[3] · Hugh M. Taylor[1] · Peter J. Nicholas[1] · Stéphane Doyen[1] · Michael E. Sughrue[1,2]

Received: 23 September 2021 / Accepted: 23 December 2021 / Published online: 4 February 2022

Abstract

Purpose Applying graph theory to the human brain has the potential to help prognosticate the impacts of intracerebral surgery. Eigenvector (EC) and PageRank (PR) centrality are two related, but uniquely different measures of nodal centrality which may be utilized together to reveal varying neuroanatomical characteristics of the brain connectome.

Methods We obtained diffusion neuroimaging data from a healthy cohort (UCLA consortium for neuropsychiatric phenomics) and applied a personalized parcellation scheme to them. We ranked parcels based on weighted EC and PR, and then calculated the difference (EP difference) and correlation between the two metrics. We also compared the difference between the two metrics to the clustering coefficient.

Results While EC and PR were consistent for top and bottom ranking parcels, they differed for mid-ranking parcels. Parcels with a high EC centrality but low PR tended to be in the medial temporal and temporooccipital regions, whereas PR conferred greater importance to multi-modal association areas in the frontal, parietal and insular cortices. The EP difference showed a weak correlation with clustering coefficient, though there was significant individual variation.

Conclusions The relationship between PageRank and eigenvector centrality can identify distinct topological characteristics of the brain connectome such as the presence of unimodal or multimodal association cortices. These results highlight how different graph theory metrics can be used alone or in combination to reveal unique neuroanatomical features for further clinical study.

Keywords Connectivity · Graph theory · Centrality · Neurosurgery

Introduction

Preserving brain function and maximizing quality of life are fundamental goals in neurosurgery. Advances in surgical methods, including intraoperative mapping, awake surgery, and neurophysiology have helped minimize post-surgical neurological deficits and improved patient outcomes [1]. These techniques attempt to identify areas of the brain which are more readily associated with observable functions to inform the surgeon of which areas should not be cut to avoid causing neurologic deficits. Previous attempts to delineate these regions, collectively referred to as "eloquent" brain [2], have commonly implemented imaging techniques such as functional magnetic resonance imaging (fMRI), but have not been widely adopted in part due to the unavailability of pipelines for clinical translation [3, 4]. Furthermore, while identifying regions largely responsible for speech or motor deficits has been helpful to preserve these functions, the neurosurgical community has maintained a less thorough familiarity with the functional deficits which occur with injury in traditionally "non-eloquent" cerebrum [5]. Ultimately, our ability to maximize post-operative morbidity has been largely limited by the lack of complete information on the brain's structural-functional architecture [6–8].

More recently, the field of network neuroscience has emerged as a transdisciplinary effort to improve our insight into the organizational principles of the brain through

✉ Michael E. Sughrue
sughruevs@gmail.com

1 Omniscient Neurotechnology, Sydney, Australia

2 Centre for Minimally Invasive Neurosurgery, Prince of Wales Hospital, Randwick, NSW 2031, Australia

3 Robert Wood Johnson Medical School, Rutgers University, New Brunswick, NJ 08901, USA

comparisons with a number of other fields studying the physics of complex systems. Analyses of the topological structure of a network have improved our understanding of information flow through electrical power grids [9], the vulnerability of IT communication networks [10], the extent of collaboration among scientists in academia [11], and about complex biological networks [12]. More recently, through improvements in big data approaches and in the availability of large datasets, it has become clear that like many complex systems, the brain "connectome" involves large-scale neural networks which are architecturally organized to maximize the global transfer and integration of information while also minimizing metabolic cost [13, 14]. In particular, applying graph theory on the brain's structural wiring diagram has provided a possible way to improve our understanding of structural-functional relationships in the brain beyond a localizationist view, as the function of a system is intricately related to the dynamic interactions of many of its structural elements [15]. According to graph theory, the structural brain network can be thought of as a series of anatomical regions, or nodes, linked by pairwise white matter connections, or edges [16]. Given the importance of spatial heterogeneity in human brain organization, anatomical regions can also be defined according to more anatomically fine, imaging based parcellation schemes in which individual parcellations represent the nodes of a graph. Despite how individual nodes may be defined, the complete set of nodes and edges of a brain graph comprises the adjacency matrix of the connectome, a model of the topology of the brain.

It is increasingly clear that at least some of the functional capacity of the brain arises from more complex multinetwork interactions and global topological characteristics, and therefore understanding brain dynamics requires measures which take into consideration the entire brain connectome and not just localized brain regions [13]. Through a graph theory approach, these characteristics can be revealed mathematically and thus can offer additional information which may be useful for neurosurgical decision making [17]. Within a network, highly influential nodes which have structural or functional significance are referred to as network "hubs" [18]. Regions more likely to be hubs can be defined based on various measurements on the network, though centrality is the most common. Centrality is the ability of a node to influence, or be influenced by other nodes as a result of its connection topology [19]. Two measures which may be used to identify hub nodes are eigenvector (EC) centrality and PageRank (PR) centrality [20]. Our group in the past has shown that PR may be a good indicator of neurosurgical eloquence [20], with significant interindividual variation to possibly justify the use of graph theory for each patient's surgical planning [7]. While EC and PR are similar measures of centrality, some important mechanistic differences exist between them, such as that PR biases against end nodes or those nodes which are just connected to just highly connected nodes unlike EC [21]. Thus, it is important to consider the differences in information these metrics reveal about the topological characteristics of the brain connectome compared to each other, and if they provide further information when used in combination.

Here, we studied a cohort of subjects who have undergone diffusion neural imaging and utilized artificial intelligence software to construct a personalized brain atlas and determined the centrality of each brain region. We sought to compare Eigenvector and PageRank centrality to derive improved meaning of these measures when studying the brain connectome. We aimed to examine what possible neuroanatomical features are revealed by the differences between these two metrics and if this difference could provide a tool for intracerebral neurosurgery worth further clinical investigation. We incorporate our results into a previously established, fine parcellation scheme by the Human Connectome Project (HCP) in order to provide an empiric basis for future study which is anatomically specific.

Methods

Data collection and pre-processing

Magnetic resonance images (MRI) consisting of diffusion tensor images (DTI) and the T1 anatomical scan of 81 healthy subjects was obtained from the UCLA Consortium for Neuropsychiatric Phenomics La5c Study from OpenNeuro (https://openneuro.org). This cohort was chosen as it is from a publicly available dataset of healthy control subjects with the purpose of examining brain function and anatomy [22]. The DTI were processed using the Omniscient software [23]. This employs standard processing steps in the Python language which have been published previously [23] and are described in brief below and in the Supplementary Methods (Supplementary Fig. 1).

Creation of a personalized brain atlas using machine learning-based parcellations

The HCP atlas [24] is based on a machine-learning classifier which parcellates the brain based on multiple modalities including resting-state fMRI, task functional fMRI, myelin content, and cortical thickness. The machine learning tool used by the Glasser scheme is however not currently publicly available and therefore only the group average from the Glasser study can be used. Global parcellations may however overlook important individual differences and therefore, subject specific application of machine learning tools is required to increase the accuracy of parcellation.

To minimize gyral variation across individuals, a machine learning based, subject specific version of the HCP-MMP1 atlas was generated using each subject's structural connectivity by warping the HCP atlas onto each individual's brain based on structural connectivity, as described by Doyen et al. [23]. This culminates in 181 cortical parcels and 8 subcortical structures per hemisphere, and the brainstem (as one parcel).

Calculation of centrality measures

The generated bi-hemispheric weighted adjacency matrices were used to calculate the graph centrality metrics using the NetworkX module in Python 3.9. Weighted PageRank Centrality, Eigenvector Centrality and Clustering Coefficient were computed for all 379 parcels.

Identified parcels were mapped to core resting-state networks based on the 7 Network Yeo-Buckner model [25]: the central executive network (CEN), default mode network (DMN), dorsal attention network (DAN), limbic network (LN), salience network (SN), sensorimotor network (SMN), and visual network (VN). The Yeo-Buckner model was chosen given its similar anatomical granularity as the Glasser parcellation scheme which allows for more fine results and better hypothesis comparison between future studies. Individual parcellations were visually mapped into each network according to anatomical borders and have since been previously reported by our team [5, 26] and found to demonstrate similar results to other network models from the HCP scheme [27].

Analysis of graph metric measures

In order to compare metrics between individuals, raw centrality scores were ranked in descending order for each subject, such that a smaller numerical rank indicated a higher nodal centrality. At the group level, the median rank, and interquartile range of ranks for each parcel was calculated to compare each metric. Spearman's correlation was performed to test for association between median ranks for each metric at the group level and individual level as these data were not normally distributed and violated assumptions for Pearson correlation. The difference between eigenvector and PageRank centrality ranks was plotted against the average of the two ranks for every parcel across the 81 subjects in a Bland-Altman plot to identify patterns in the difference between the two measures. The biggest differences between median eigenvector and PageRank centrality were then calculated, and the top 30 parcels with either higher PR or higher EC were tabulated. Pairwise Mann-Whitney U Tests were performed to compare PR and EC for each parcel within a given network across individuals. A derivative measure, the eigenvector-PageRank difference (EP difference) was calculated for each parcel and ranked in each individual. The EP difference and clustering coefficient were next transformed into categorical variables through division into tertiles (high: ranks 1–126, mid: ranks 127–253, low: ranks 245–379). A chi-square test of association and a post-hoc Cramer's V were performed on the rank of every parcel for each individual (30,699 ranks). Post-hoc pairwise Chi-square analyses between each group was performed and standardized residuals and Bonferroni-corrected p values were calculated to identify group differences. Heatmaps were generated for each measure to discern patterns across individuals. All analysis was performed in R version 4.1.2.

Results

Subject demographics

The average age (±SD) for the 81 participants was 27 ± 6.75. 42 (51.9%) were female, and 39 (48.1%) were male. All participants were right-handed. Additional available demographic data were limited.

PageRank centrality and eigenvector centrality identify distinct regions

Median eigenvector and PageRank ranks showed a strong positive correlation ($\rho = 0.83$, $p < 0.001$), though there were clear outliers (Fig. 1a). A Bland-Altman plot of the ranks of the two measures for each parcel across 81 individuals showed a diamond shape with a mean difference of 0 ± 181.9 (Fig. 1b). The bias of 0 was likely due to each measure sometimes being higher than the other, and the wide limits of agreement suggest a considerable degree of discrepancy. Nonetheless, the two measures tended to diverge at middle-ranking parcels, suggest discrepancy, while parcels at the extreme ranks (top or bottom ranks) tended to have a similar PageRank and eigenvector.

When the EC and PR ranks for each parcel were split by the core network affiliation of each parcel for all 81 subjects, pairwise Mann-Whitney U tests revealed a significant difference in EC and PR in the visual ($W = 8{,}558{,}458$, $p < 0.001$) and limbic networks ($W = 1{,}670{,}178$, $p < 0.001$), with higher EC rank than PR. In contrast, parcels in the CEN ($W = 13{,}121{,}829$, $p < 0.001$), DMN ($W = 23{,}176{,}330$, $p < 0.001$), and SN ($W = 8{,}586{,}528$, $p < 0.001$) tended to have a greater PR than EC (Fig. 1c). Subcortical structures tended to rank higher than parcels in other networks. The wide whiskers of the plots indicated a high level of interindividual variability, making it difficult to discern meaningful group-level patterns.

The interindividual variation became clear when we plotted PageRank and eigenvector for all 81 subjects

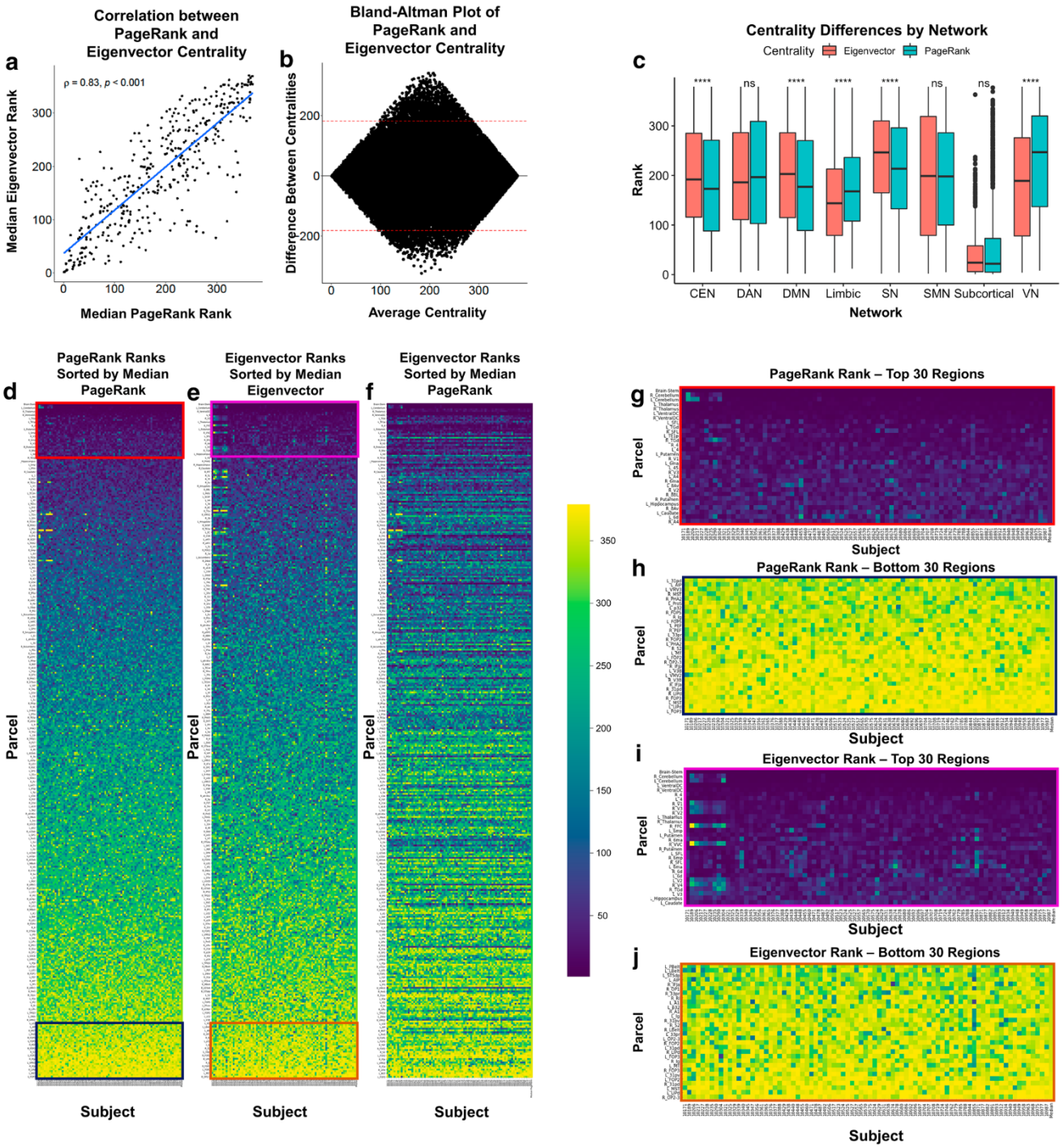

in a heatmap, ordered by the respective median rank (Fig. 1d–f). Top and bottom-ranking parcels were visually consistent across individuals (Fig. 1g–j), whereas most variation was qualitatively seen in the middle of the heatmap (Fig. 1d–f). Ranking eigenvector by the median PageRank in a heatmap highlighted the disparity between the two measures, with a "banding" effect consistent with parcels ranking higher in eigenvector than PageRank (Fig. 1f).

Differences between PageRank and eigenvector centralities

The difference between the ranks of the PageRank and eigenvector centralities for each parcel were calculated to identify the most discrepant parcels between the two measures. A heatmap of the ranked differences between eigenvector and PageRank (EP difference) showed some interindividual variation in terms of the degree to which the two centralities differed

◂**Fig. 1** Comparing eigenvector and PageRank centrality. **a** Median PageRank and eigenvector rank of all 379 parcels from 81 subjects showed a strong positive correlation. **b** A Bland-Altman plot of the average of the two values against the difference between the two values for each parcel across 81 subjects (30,699 data points) demonstrated a diamond shape with a mean difference of 0 ± 181.9. **c** A boxplot comparing eigenvector and PageRank ranks by network affiliations, plotted using all 30,699 data points, revealed insignificant differences between the two measures by network. **d** A heatmap of the PageRank rank for all 379 parcels across 81 subjects, ranked by the median PageRank rank of each parcel, from the highest ranking (blue) to lowest (yellow). **e** A heatmap of the eigenvector rank for all 379 parcels across 81 subjects, ranked by the median eigenvector rank of each parcel, from the highest ranking (blue) to lowest (yellow). **f** A heatmap of the eigenvector rank for all 379 parcels across 81 subjects, ranked by the median PageRank rank of each parcel, from the highest ranking (blue) to lowest (yellow). Zoomed in views of the top and bottom of the heatmaps of PageRank rank (**g–h**) and eigenvector rank (**i–j**) are provided to demonstrate a closer view of any the amount variation specifically for the top and bottom 30 parcels for each measure. p-values in panel a represent correlations between metrics studied. *CEN* central executive network; *DAN* dorsal attention network; *DMN* default mode network; *LN* limbic network; *SC* subcortical network; *SMN* sensorimotor network; *SN* salience network; *VN* visual network

for each parcel (Fig. 2a), though parcels at each extreme were again largely consistent. To confirm this, we ranked the median EP difference for the 379 parcels and plotted this against the IQR of the EP difference for each parcel (Fig. 2b). This produced a parabolic plot showing an increase in variability of EP difference for the middle ranking parcels, whereas parcels with the highest and lowest median EP difference had lower variability ($R^2 = 0.32$).

Looking at the top 30 discrepant parcels (Table 1), parcels in the VN, LN, SMN, and specific aspects of the DMN had higher Eigenvector centrality compared to PageRank (Fig. 2c). Higher values of eigenvector centrality suggests these parcels demonstrated more connecting paths to regions which be also of high degree (i.e., to highly connected regions). Anatomically, these parcels tended to be located in primary/unimodal areas within parietal, medio-temporal and temporooccipital regions (Fig. 2d). Ten parcels in the top 30 were only present unilaterally.

In contrast, parcels which had higher PageRank compared to eigenvector centrality were in the Auditory SMN, CEN, SN, DAN, and to a lesser extent in the SMN (Fig. 2e). Anatomically, these regions tended to be located in multi-modal association areas within the temporal, insular, supramarginal, cingulate, and frontal cortices (Fig. 2f). Out of the top 30, 9 parcels were present bilaterally, while 12 parcels were only left-sided.

Relationship between EP difference and clustering coefficient

Parcels with a high EP difference are regions with a high number of connections which may be with high degree nodes (high eigenvector), but when these connections are scaled by the degree of their neighbors, their PageRank centrality is reduced. We hypothesized that these parcels may potentially be redundant regions of the brain – parcels which could be sacrificed in surgery without inflicting noticeable damage, or with a high potential for functional recovery. In order to better understand this, we calculated the clustering coefficient for each parcel across all patients, and ranked the clustering coefficient of each parcel for each individual (Fig. 3a). The clustering coefficient is a measure of how many alternative paths exist between the neighbors of a given parcel. Tracts can potentially easily bypass a parcel with a high clustering coefficient, as its neighbors provide alternative paths for information flow.

Right V8 and right EC had the highest median clustering coefficient in our cohort and the relationship between clustering coefficient and EP difference was inconsistent (Fig. 3b–c). At a group level however, median EP difference rank showed a weak positive correlation with median clustering coefficient rank ($\rho = 0.25$, $p < 0.001$) (Fig. 3d). Given the individual variability of the EP difference, we performed correlations between EP difference and clustering coefficient for each individual. The average (±SD) Spearman correlation was 0.18 ± 0.08 ($p < 0.001$), though across individuals, it ranged from 0.01 to 0.35. When repeating the analysis for the top 100 parcels with the highest median EP difference, a stronger positive correlation was found at the group level ($\rho = 0.50$, $p < 0.001$) (Fig. 3e).

Finally, EP difference rank and clustering coefficient rank were associated ($X^2 = 770.08$, $p < 0.001$) when they were categorized into tertiles. The strength of this association was however weak with a Cramer's V of 0.112. Post-hoc pairwise chi-square tests between each tertile of EP difference and clustering coefficient nonetheless demonstrated significant associations between most groups (Table 2). The greatest residual value was for the association between the lowest clustering coefficient tertile and lowest EP difference tertile, suggesting that this pair contributed most to the overall significance of the omnibus Chi-square test. This was followed by the residual value for the association between the highest tertile for both variables, suggesting that there was a greater number of parcels in the highest tertiles of EP difference and clustering coefficient than would be expected by chance, with 43.5% of parcels in the highest tertile of clustering coefficient also having an EP difference in the highest tertile. Plotting this relationship (Fig. 3f) demonstrated a trend of decreasing number of parcels in the highest tertile of

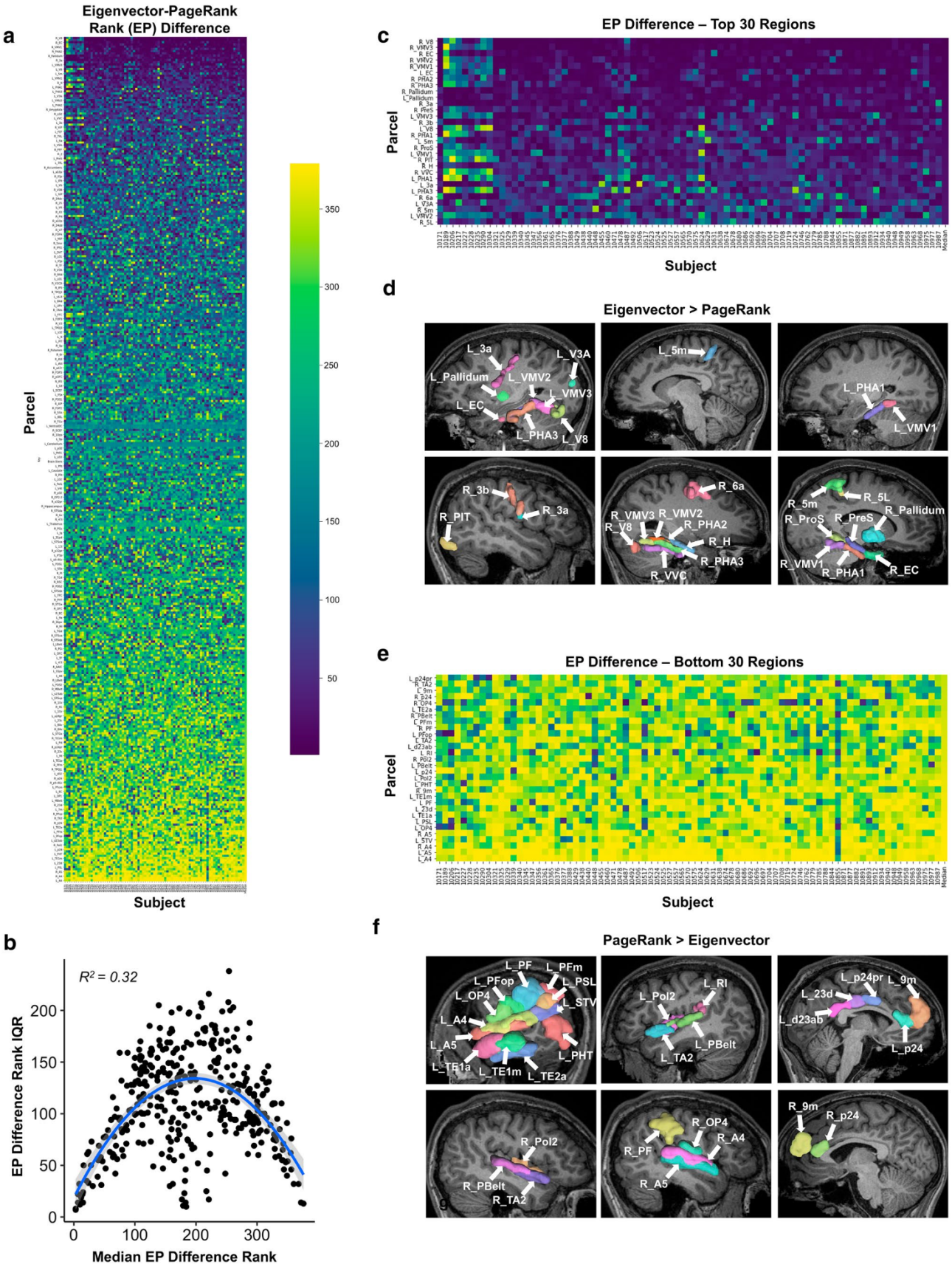
a
Eigenvector-PageRank
Rank (EP) Difference
Parcel
Subject
350
300
250
200
150
100
50
b
$R^2 = 0.32$
EP Difference Rank IQR
Median EP Difference Rank
0
50
100
150
200
0
100
200
300
c
EP Difference – Top 30 Regions
Parcel
Subject
d
Eigenvector > PageRank
L_3a
L_V3A
L_Pallidum
L_VMV2
L_VMV3
L_EC
L_PHA3
L_V8
L_5m
L_PHA1
L_VMV1
R_3b
R_3a
R_PIT
R_6a
R_VMV3
R_VMV2
R_V8
R_PHA2
R_H
R_PHA3
R_VVC
R_5m
R_5L
R_Pallidum
R_ProS
R_PreS
R_VMV1
R_PHA1
R_EC
e
EP Difference – Bottom 30 Regions
Parcel
Subject
f
PageRank > Eigenvector
L_PF
L_PFm
L_PFop
L_PSL
L_OP4
L_STV
L_A4
L_A5
L_TE1a
L_TE1m
L_TE2a
L_PHT
L_Pol2
L_RI
L_PBelt
L_TA2
L_23d
L_p24pr
L_9m
L_d23ab
L_p24
R_Pol2
R_PBelt
R_TA2
R_OP4
R_A4
R_PF
R_A5
R_9m
R_p24

◂**Fig. 2** Investigating the eigenvector-PageRank difference. **a** A heatmap of the difference between the eigenvector rank and the PageRank rank (EP difference), which is itself ranked from 1-379 ("1" being the parcel with a high eigenvector rank but low PageRank rank, in blue, and "379" a parcel with a high PageRank rank but low eigenvector rank, in yellow). **b** A plot of median EP difference rank against their interquartile range for each parcel demonstrated a parabolic shape, indicative of increasing variability for mid-ranking parcels. **c** Top 30 parcels with the highest EP difference showed little individual variation. **d** These parcels tended to be in the medial temporal and temporooccipital regions bilaterally. **e** Bottom 30 parcels, or those with the highest PE difference (high PageRank low eigenvector) demonstrated some variation but this was still more consistent than for middle ranking parcels. **f** Anatomically, parcels with the highest PE difference tended to be perisylvian, insular and cingulate structures

clustering coefficient moving from the highest EP difference tertile to the lowest. Therefore, while EP difference is clearly different from clustering coefficient, there was some relationship between the two measures in our cohort for the regions with the highest or lowest EP differences, which also varies greatly between individuals.

Discussion

Damage to traditionally defined eloquent regions does not always lead to impairment, while in other patients, focal lesions of areas that would not be defined as eloquent can lead to unexpected cognitive deficits not associated with that region's functionality [28–30]. Consequently, there is a need to continually assess measures which may improve our modelling of brain activity on an individual level, possibly from a network perspective. Here, we present data that two graph theory measures, PageRank (PR) and eigenvector (EC) centrality, can reveal important neuroanatomical features of the brain connectome with some unique differences which may be revealed when studied together. Areas of high EC and low PR could better identify primary and unimodal association areas compared to areas of high PR and low EC which seemed to favor more integrative, multimodal association cortices. While we hypothesized that the mismatch between these two metrics ("EP difference") could identify possibly redundant areas of the brain, a relatively weak relationship was found between EP difference and clustering coefficient suggesting that EP difference may not be optimal to identify individual parcellations which are surrounded by an increased number alternate paths. The current results, while purely theoretical, highlight the feasibility of examining varying graph theory metrics in combination to reveal unique topological characteristics of the brain connectome related to topics of immense interest in the neurosurgical field, such as eloquence and redundancy.

Differences between PageRank and eigenvector

Applying different measures of centrality, or only relying on degree centrality, is a common technique described in the literature to identify hub nodes [15, 31]. In particular, both eigenvector (EC) and PageRank (PR) centrality have been well described mathematically [32–34]. They are closely related measures which can identify hub regions but with some important mechanistic differences: EC places more importance on nodes which are connected to more highly connected nodes, while PR is a is a derivative of EC which which scales the influence of incoming connections by how popular those sender nodes are. In other words, PR biases against nodes with a single connection to a high degree node unlike EC [20]. PR is in fact designed to be used for directed networks, though it can also be used for assessing centrality based on brain connectivity by treating a brain graph as a directed network with bidirectional edges [35]. While PR seems to provide clinically valuable information about more unique brain regions [7, 20], the differences in behavior between EC and PR need to be examined biologically with the goal of clinical application, rather than just mathematically. However, the limited understanding of the neuroanatomical features of these measures has prevented their widespread acknowledgement and clinical study in fields such as neurosurgery to date.

Areas of high eigenvector or PageRank centrality

Higher EC compared to PR may indicate the presence of primary/unimodal association cortices which are involved in immediate sensory input. We found these regions generally included several parts of the visual and limbic networks as well as some parahippocampal regions [36]. Visual areas found in the highest quintile of eigenvector centrality (areas R_V8, R_VMV1, R_PIT and R_VVC) are all located in the basal surface of the occipital lobe, and are all connected through the vertical occipital fasciculus (VOF) as previously shown [37]. The VOF connects the dorsal and ventral visual streams and is thought to be crucial for visual processing as it integrates the visual cortex. Interestingly, Jitsuishi et al. found that the VOF's fiber tracts are rightward lateralized [16], which may be consistent with the slightly higher eigenvector ranks of the right visual parcellations in the current work. Similarly, the superficial layers of the entorhinal cortex of the limbic network are thought to send information to more multi-modal association areas of the medial temporal cortices, like the hippocampal formation, for memory formation and consolidation [38]. While there are limited studies on the effects of lesions to the entorhinal cortex in humans, the parahippocampal cortices demonstrate a similar role, and damage to parahippocampal cortices has been associated

Table 1 Differences in mean eigenvector centrality and PageRank centrality (parcels with a rank of at least 80 in either metric bolded)

PageRank and eigenvector							
Higher PageRank				Higher eigenvector			
Parcellation	Network	PageRank rank	Eigenvector rank	Parcellation	Network	PageRank rank	Eigenvector rank
L_A4	Auditory	31	214	**R_V8**	Visual	298	66
L_A5	Auditory	72	227	R_VMV3	Visual	320	97
R_A4	Auditory	36	175	**R_EC**	Limbic	273	76
L_STV	DMN	139	262	R_VMV2	Visual	338	152
R_A5	Auditory	79	197	**R_VMV1**	Visual	260	78
L_OP4	Sensorimotor	132	248	L_EC	Limbic	261	88
L_PSL	Auditory	148	262	R_PHA2	DMN	345	184
L_TE1a	DMN	45	158	R_PHA3	DMN	332	180
L_PF	DAN	58	170	R_Pallidum	Subcortical	241	90
L_23d	CEN	165	277	L_Pallidum	Subcortical	247	97
L_TE1m	CEN	54	163	R_3a	Sensorimotor	243	97
R_9m	DMN	48	154	R_PreS	DMN	321	184
L_PHT	Language/DAN	66	172	L_VMV3	Visual	341	207
L_PoI2	Salience	94	196	**R_3b**	Sensorimotor	209	80
L_p24	CEN	202	303	L_V8	Visual	217	93
L_PBelt	Language/auditory	232	332	**R_PHA1**	DMN	161	43
R_PoI2	Salience	64	163	L_5m	Sensorimotor	232	118
L_RI	Auditory	192	291	R_ProS	Visual	337	228
L_d23ab	DMN	208	307	L_VMV1	Visual	305	199
L_TA2	DMN	228	325	**R_PIT**	Visual	148	48
L_PFop	Salience	152	247	R_H	Subcortical	283	187
L_PFm	CEN/language	43	133	**R_VVC**	Visual	112	21
R_PF	DAN	75	165	**L_PHA1**	DMN	169	79
R_PBelt	Auditory	219	308	L_PHA3	DMN	189	100
L_TE2a	CEN	63	147	L_3a	Sensorimotor	244	155
R_OP4	Sensorimotor	138	222	L_V3A	Visual	223	140
R_p24	CEN	216	300	R_6a	Sensorimotor	257	174
L_9m	DMN	55	138	**R_5m**	Sensorimotor	154	75
R_TA2	DMN	191	272	**R_5L**	Sensorimotor	132	58
L_p24pr	Salience	213	294	L_VMV2	Visual	365	291

with impairment in visuospatial memory [39], independent of damage to the hippocampus.

Many of the above regions have been recently described as lower in a proposed hierarchy for the cortical organization of large-scale connectivity for cognition. As defined by Margulies et al. [36], a primary/unimodal-transmodal gradient of cortical processing may exist in order to appropriately process transmodal information after immediate sensory input. At one end of this spectrum lies primary/unimodal regions, which are often connected to higher regions for multimodal integration, however, are surrounded by regions with similar roles in unimodal processing. Based on this model, high EC and low PR most closely indicated the presence of lower primary/unimodal association regions, such as occipital visual regions and regions in or bordering the parahippocampal cortices. While damage to these regions may lead to cognitive deficits, they are not often areas considered eloquent in neurosurgery as they do not lead to gross functional impairment or may be more amendable to compensatory takeover by analogue regions.

Differently, areas of high PR and low EC best identified parcellations which are often located in more multi-modal association cortices. Specifically, these parcellations are often described as part of the higher canonical resting state networks (DMN, CEN, SN), which the other networks generally align themselves in order to subserve complex cognitive functions [5, 36]. For instance, numerous temporal regions were identified (e.g., areas TE1a, TE1m and TE2a)

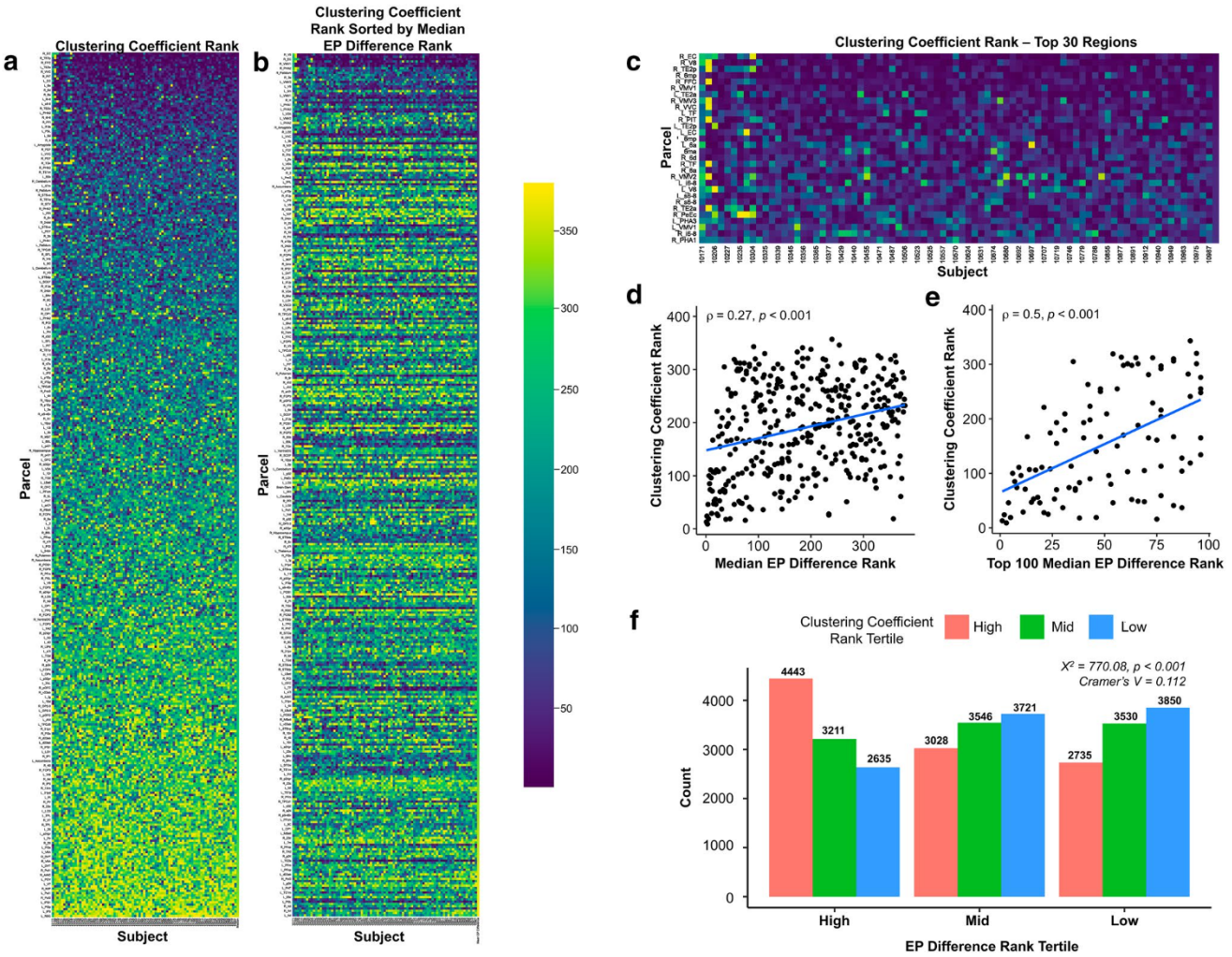

Fig. 3 Comparing EP difference and clustering coefficient. **a** A heatmap of the clustering coefficient rank for all 379 parcels across 81 subjects, ranked by the median clustering coefficient rank of each parcel, from the highest ranking (blue) to lowest (yellow). **b** A heatmap of the clustering coefficient rank for all 379 parcels across 81 subjects, ranked by the median EP difference rank of each parcel, from the highest ranking (blue) to lowest (yellow). **c** A zoomed in view of clustering coefficient rank for the top 30 regions as ranked by median clustering coefficient of each parcel is provided to demonstrate a closer view of the amount of variation. The relationship between median EP difference rank and median clustering coefficient rank for all regions (**d**) and only the top 100 regions (**e**). **f** Chi-square analysis of EP rank tertile according to clustering coefficient rank tertiles. p-values in panel d-e represent correlations between metrics studied and p-values in panel f are for chi-square analyses

which have been implicated in visual working memory and storing multimodal semantic representations after basic visual processing in the occipital visual areas [40]. Other areas identified, such as area 9 m of the superior frontal gyrus [41], area Pol2 of the posterior insula [42], and area PFm of the lateral parietal lobe [43], have all also demonstrated important roles in the complex functions like memory and language. Our team has previously found that regions of high PageRank centrality associates closely with what neurosurgeons have traditionally considered "eloquent" according to the Spetzler-Martin arteriovenous malformations classification system [2], more so than eigenvector centrality [20]. However, few studies have correlated these analyses with clinical outcomes and as such these hypotheses remain purely speculative.

Combining EC and PC measures together: the EP difference

While EC and PC measures demonstrated a high degree of similarity in top and bottom ranking parcels as expected, we hypothesized that using these two measures together ("EP difference") may offer complementary information with distinct neuroanatomical functions which is of clinical utility. According to this model (Fig. 4), regions which have high eigenvector centrality, but low PageRank centrality (high

Table 2 The EP difference and clustering coefficient were next transformed into categorical variables through division into tertiles (high: ranks 1–126, Mid: ranks 127–253, Low: ranks 245–379)

EP difference rank tertile	Clustering coefficient rank tertile		
	Low	Mid	High
Low			
Column %	37.7	34.3	26.8
Std. Res	26.2	− 6.1	− 20.2
Adj. p-value	< 0.001	< 0.001	< 0.001
Mid			
Column %	36.5	34.5	29.7
Std. Res	− 10.1	2.5	7.7
Adj. p-value	< 0.001	0.124	0.003
High			
Column %	25.8	31.2	43.5
Std. Res	− 16.2	3.6	12.6
Adj. p-value	< 0.001	< 0.001	< 0.001

EP difference) may be areas of high connectivity specifically to more connected nodes which integrate information from a number of other regions, given that they have low PageRank which biases against these connections. Therefore, high EP measurements could theoretically reflect high levels of degeneracy. In other words, since they are largely unimodal/primary modal areas that connect to integrative multi-modal areas, but do not partake in multimodal processing, then functional compensation may occur by bypassing these regions if damaged. Alternatively, a region with a low EP difference may reflect nodes with more unique connections and not just to highly connected nodes, or other integrative areas. Therefore, these regions may be considered "eloquent" [7, 20], as despite having fewer influential connections, these connections possibly facilitate important functions after integrating information from a number of regions.

However, while we found that some areas with the highest EP difference also tended to have an increased number of alternative paths between their neighbors (high clustering coefficient), the relationship was relatively weak at the group level and had significant variation on an interindividual basis. A measure which can identify regions with a high level of redundancy would be of immense interest in the neurosurgical community as it could identify candidates for neuroplastic recovery, either through neurorehabilitation or transcranial magnetic stimulation (TMS). Although, the current results do not support EP difference in its current form as such a clinical tool. Further investigations are necessary to determine the information provided by the EP difference, and these should evaluate other measures of redundancy which may be better candidates for assessing this relationship.

Hubness as a measure of eloquence

The diversity of responses to focal lesions in neurosurgery suggest that resulting impairments across a variety of cognitive domains may be explained by extending the definition of "eloquence" to "hubness". Hub regions demonstrate greater susceptibility to neurological disease, and simultaneously when disease impinges on these regions, there is greater ensuing damage. Hub nodes make several long-distance connections which are susceptible to injury; they lie on many shortest paths [44], allowing pathology to spread easily to these nodes [45]; and they may have higher metabolic requirements [46], making them susceptible to metabolic stress. Furthermore, as an empiric measure, cognitive recovery of patients with ischemic stroke was predicted using a score of the extent to which hub nodes were affected [47]. Infarcts in hub regions were associated with reduced global efficiency, while strokes in non-hub regions were predictors of better cognitive function one year after stroke. Further clinical studies are however required to compare centrality measures and arrive at a consortium definition of hubness for clinical practice.

Clinical translation and future directions

Our data raise the need for further investigation into the meaning and surgical utility of centrality measures. It is however difficult to judge the utility of these measures without clinical studies. While the EP difference shows some trends in healthy individuals, it also demonstrates a significant level of variability, and given our limited sample size, it is not possible to derive clinical meaning to this metric without surgical studies. Although the degree to which the current results support further clinical study is limited. Furthermore, although graph theory can be done on individuals whose neuroanatomy is distorted by complex brain tumors, our cohort did not include individuals with diverse pathology. For instance, varying tumor types and tumor locations may impact the way EC and PR models specific neuroanatomic substrates and their interconnecting paths, which may further alter structure-function relationships in the brain like redundancy, degeneracy, and eloquence differently [48]. Therefore, our inferences about the utility of these measures in patients with brain tumors remains purely speculative.

Hypotheses from the current study were largely motivated by the desire to expand our understanding of transdisciplinary tools like graph theory which can model neuroanatomical features of the brain connectome and ultimately be used in neurosurgery. While our work may provide an empiric and hypothetical basis which may assist others in expanding the clinical utility of these tools in the future, our results are far from capable of currently informing current neurosurgical decisions. Importantly, some

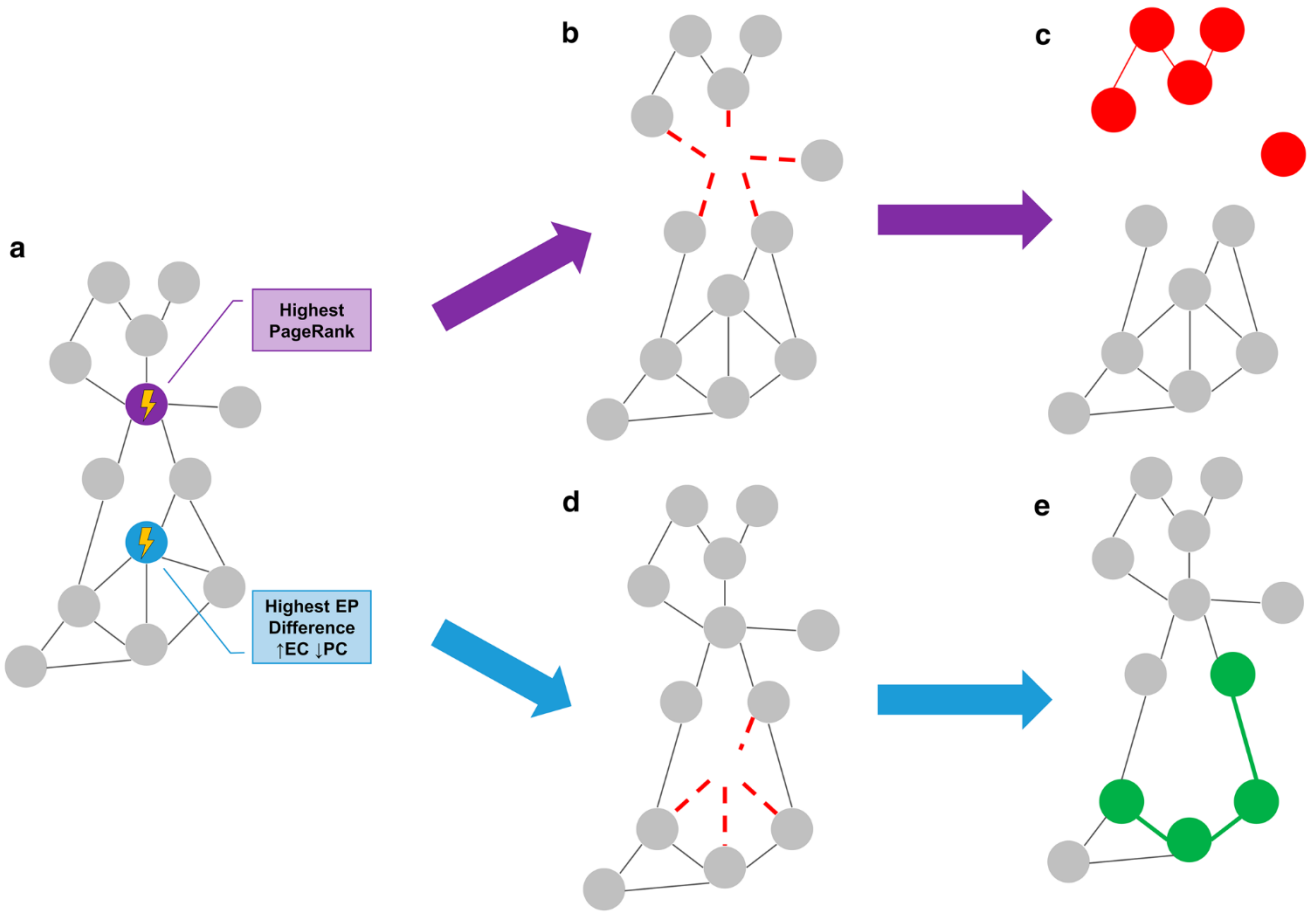

Fig. 4 EP difference to predict neurological redundancy. An example of an undirected, unweighted graph is demonstrated to model how EP difference may be utilized clinically (**a**). The purple node is the parcel with the highest PageRank, whereas the blue node has the highest EP difference, with the highest Eigenvector centrality in the network. In the top path, when the purple node is damaged (**b**), the connections to its neighbors are subsequently disrupted, and may be further damaged through retrograde degeneration (red), **c** subsequently jeopardizing a large proportion of the network and the transfer of information. In contrast, if the blue node is damaged (**d**), while the connections to its neighbors may be disrupted, information can bypass this node and still reach the other end of the network. **e** The connections of the surrounding nodes may be strengthened, and a functional compensation can occur by the neighboring nodes (green). *EP Difference* eigenvector-PageRank difference; *EC* eigenvector centrality; *PC* PageRank centrality

graph theory metrics may not yet be completely optimized for analysis with undirected brain networks despite any mechanistic fitting. Logically, there is a strong need to next link many graph theory measures in retrospective clinical studies to understand how strongly they correspond with clinical substrates in pathological specimens.

Supplementary Information The online version contains supplementary material available at https://doi.org/10.1007/s11060-021-03935-z.

Author contributions OT, SD and MES contributed to the study conception and design. Material preparation, data collection and analysis were performed by HMT, PJN, and OT. The first draft of the manuscript was written by OT and IMY and all authors commented on previous versions of the manuscript. The edited and revised draft of the manuscript was written by ND and OT. All authors read and approved the final manuscript.

Funding No funding was received for conducting this study.

Data availability The authors declare that the data supporting the findings of this study are available within the article and its supplementary information files.

Code availability The code and software used in the current study is proprietary.

Declarations

Conflict of interest Isabella M. Young, Hugh M. Taylor, Peter J. Nicholas, Stéphane Doyen, and Michael E. Sughrue are employees of and shareholders in Omniscient Neurotechnology. Onur Tanglay is an employee of Omniscient Neurotechnology. Nicholas B. Dadario has no disclosures.

Ethical approval The data used in the study are from a publicly available dataset. The procedures in the original study were approved by the Institutional Review Boards at UCLA and the Los Angeles Country Department of Mental Health.

References

1. Hervey-Jumper SL, Li J, Lau D, Molinaro AM, Perry DW, Meng L, Berger MS (2015) Awake craniotomy to maximize glioma resection: methods and technical nuances over a 27-year period. J Neurosurg 123:325–339. doi:https://doi.org/10.3171/2014.10.Jns141520
2. Spetzler RF, Martin NA (1986) A proposed grading system for arteriovenous malformations. J Neurosurg 65:476–483. doi:https://doi.org/10.3171/jns.1986.65.4.0476
3. Stopa BM, Senders JT, Broekman MLD, Vangel M, Golby AJ (2020) Preoperative functional MRI use in neurooncology patients: a clinician survey. NeuroSurg Focus 48:E11. doi:https://doi.org/10.3171/2019.11.Focus19779
4. Silva MA, See AP, Essayed WI, Golby AJ, Tie Y (2018) Challenges and techniques for presurgical brain mapping with functional MRI. NeuroImage Clin 17:794–803. https://doi.org/10.1016/j.nicl.2017.12.008
5. Dadario NB, Brahimaj B, Yeung J, Sughrue ME (2021) Reducing the cognitive footprint of brain tumor surgery. Front Neurol 12:711646. https://doi.org/10.3389/fneur.2021.711646
6. Mandonnet E, Cerliani L, Siuda-Krzywicka K, Poisson I, Zhi N, Volle E, De Schotten M (2017) A network-level approach of cognitive flexibility impairment after surgery of a right temporo-parietal glioma. Neurochirurgie 63:308–313
7. Yeung JT, Taylor HM, Young IM, Nicholas PJ, Doyen S, Sughrue ME (2021) Unexpected hubness: a proof-of-concept study of the human connectome using pagerank centrality and implications for intracerebral neurosurgery. J Neurooncol 151:249–256. doi:https://doi.org/10.1007/s11060-020-03659-6
8. Duffau H, Moritz-Gasser S, Mandonnet E (2014) A re-examination of neural basis of language processing: proposal of a dynamic hodotopical model from data provided by brain stimulation mapping during picture naming. Brain Lang 131:1–10. doi:https://doi.org/10.1016/j.bandl.2013.05.011
9. Zhou S (2021) Research on local topology tracking of power grid based on graph theory. Secur Commun Netw 2021:7027907. https://doi.org/10.1155/2021/7027907
10. Alonso M, Turanzas J, Amaris H, Ledo AT (2021) Cyber-physical vulnerability assessment in smart grids based on multilayer complex networks. Sensors. https://doi.org/10.3390/s21175826
11. Newman MEJ (2001) The structure of scientific collaboration networks. Proc Natl Acad Sci 98:404–409. https://doi.org/10.1073/pnas.98.2.404
12. Jeong H, Tombor B, Albert R, Oltvai ZN, Barabási A-L (2000) The large-scale organization of metabolic networks. Nature 407:651–654
13. Bullmore E, Sporns O (2009) Complex brain networks: graph theoretical analysis of structural and functional systems. Nat Rev Neurosci 10:186–198. doi:https://doi.org/10.1038/nrn2575
14. Briggs RG, Conner AK, Baker CM, Burks JD, Glenn CA, Sali G, Battiste JD, O'Donoghue DL, Sughrue ME (2018) A connectomic Atlas of the human cerebrum-chapter 18: the connectional anatomy of human brain networks. Oper Neurosurg 15:S470–S480. https://doi.org/10.1093/ons/opy272
15. Rubinov M, Sporns O (2010) Complex network measures of brain connectivity: uses and interpretations. NeuroImage 52:1059–1069. https://doi.org/10.1016/j.neuroimage.2009.10.003
16. Farahani FV, Karwowski W, Lighthall NR (2019) Application of graph theory for identifying connectivity patterns in human brain networks: a systematic review. Front Neurosci 13:585. https://doi.org/10.3389/fnins.2019.00585
17. Hart MG, Ypma RJF, Romero-Garcia R, Price SJ, Suckling J (2016) Graph theory analysis of complex brain networks: new concepts in brain mapping applied to neurosurgery. J Neurosurg 124:1665–1678. https://doi.org/10.3171/2015.4.JNS142683
18. van den Heuvel MP, Sporns O (2011) Rich-club organization of the human connectome. J Neurosci 31:15775–15786
19. Oldham S, Fulcher B, Parkes L, Arnatkevičiūtė A, Suo C, Fornito A (2019) Consistency and differences between centrality measures across distinct classes of networks. PLoS ONE 14:e0220061. doi:https://doi.org/10.1371/journal.pone.0220061
20. Ahsan SA, Chendeb K, Briggs RG, Fletcher LR, Jones RG, Chakraborty AR, Nix CE, Jacobs CC, Lack AM, Griffin DT, Teo C, Sughrue ME (2020) Beyond eloquence and onto centrality: a new paradigm in planning supratentorial neurosurgery. J Neurooncol 146:229–238. doi:https://doi.org/10.1007/s11060-019-03327-4
21. Senanayake U, Piraveenan M, Zomaya A (2015) The pagerank-index: going beyond citation counts in quantifying scientific impact of researchers. PLoS ONE 10:e0134794
22. Gorgolewski K, Durnez J, Poldrack R (2017) Preprocessed consortium for neuropsychiatric phenomics dataset. F1000Res. https://doi.org/10.12688/f1000research.11964.2
23. Doyen S, Nicholas P, Poologaindran A, Crawford L, Young IM, Romero-Garcia R, Sughrue ME (2021) Connectivity-based parcellation of normal and anatomically distorted human cerebral cortex. Hum Brain Mapp. doi:https://doi.org/10.1002/hbm.25728
24. Glasser MF, Coalson TS, Robinson EC, Hacker CD, Harwell J, Yacoub E, Ugurbil K, Andersson J, Beckmann CF, Jenkinson M, Smith SM, Van Essen DC (2016) A multi-modal parcellation of human cerebral cortex. Nature 536:171–178. doi:https://doi.org/10.1038/nature18933
25. Yeo BTT, Krienen FM, Sepulcre J, Sabuncu MR, Lashkari D, Hollinshead M, Roffman JL, Smoller JW, Zöllei L, Polimeni JR, Fischl B, Liu H, Buckner RL (2011) The organization of the human cerebral cortex estimated by intrinsic functional connectivity. J Neurophysiol 106:1125–1165. doi:https://doi.org/10.1152/jn.00338.2011
26. Sandhu Z, Tanglay O, Young IM, Briggs RG, Bai MY, Larsen ML, Conner AK, Dhanaraj V, Lin YH, Hormovas J, Fonseka RD, Glenn CA, Sughrue ME (2021) Parcellation-based anatomic modeling of the default mode network. Brain Behav 11:e01976. doi:https://doi.org/10.1002/brb3.1976
27. Akiki TJ, Abdallah CG (2019) Determining the hierarchical architecture of the human brain using subject-level clustering of functional networks. Sci Rep 9:19290. https://doi.org/10.1038/s41598-019-55738-y
28. Coomans MB, van der Linden SD, Gehring K, Taphoorn MJB (2019) Treatment of cognitive deficits in brain tumour patients: current status and future directions. Curr Opin Oncol 31:540–547. doi:https://doi.org/10.1097/CCO.0000000000000581
29. Duffau H, Capelle L, Denvil D, Sichez N, Gatignol P, Lopes M, Mitchell M-C, Sichez J-P, Van Effenterre P (2003) Functional recovery after surgical resection of low grade gliomas in eloquent brain: hypothesis of brain compensation. J Neurol Neurosurg Psychiatr 74:901–907. https://doi.org/10.1136/jnnp.74.7.901
30. Herbet G (2021) Should complex cognitive functions be mapped with direct electrostimulation in wide-awake surgery? A network perspective. Front Neurol. https://doi.org/10.3389/fneur.2021.635439
31. Sporns O (2018) Graph theory methods: applications in brain networks. Dialogues Clin Neurosci 20:111–121. doi:https://doi.org/10.31887/DCNS.2018.20.2/osporns

32. Hansen DL, Shneiderman B, Smith MA, Himelboim I (2020) Chapter 3—social network analysis: measuring, mapping, and modeling collections of connections. In: Hansen DL, Shneiderman B, Smith MA, Himelboim I (eds) Analyzing social media networks with NodeXL, 2nd edn. Morgan Kaufmann, Burlington, pp 31–51
33. Brin S, Page L (1998) The anatomy of a large-scale hypertextual web search engine. Comput Netw ISDN Syst 30:107–117. https://doi.org/10.1016/S0169-7552(98)00110-X
34. Bonacich P (1972) Factoring and weighting approaches to status scores and clique identification. J Math Sociol 2:113–120. doi:https://doi.org/10.1080/0022250X.1972.9989806
35. Zuo X-N, Ehmke R, Mennes M, Imperati D, Castellanos FX, Sporns O, Milham MP (2011) Network centrality in the human functional connectome. Cereb Cortex 22:1862–1875. https://doi.org/10.1093/cercor/bhr269
36. Margulies DS, Ghosh SS, Goulas A, Falkiewicz M, Huntenburg JM, Langs G, Bezgin G, Eickhoff SB, Castellanos FX, Petrides M, Jefferies E, Smallwood J (2016) Situating the default-mode network along a principal gradient of macroscale cortical organization. Proc Natl Acad Sci 113:12574–12579. https://doi.org/10.1073/pnas.1608282113
37. Baker CM, Burks JD, Briggs RG, Stafford J, Conner AK, Glenn CA, Sali G, McCoy TM, Battiste JD, O'Donoghue DL, Sughrue ME (2018) A connectomic Atlas of the human cerebrum-chapter 9: the occipital lobe. Oper Neurosurg 15:S372–S406. https://doi.org/10.1093/ons/opy263
38. Insausti R, Amaral D (2004) Hippocampal formation. Hum Nerv Syst 2:871–914
39. Aminoff EM, Kveraga K, Bar M (2013) The role of the parahippocampal cortex in cognition. Trends Cogn Sci 17:379–390. doi:https://doi.org/10.1016/j.tics.2013.06.009
40. Visser M, Jefferies E, Embleton KV, Lambon Ralph MA (2012) Both the middle temporal gyrus and the ventral anterior temporal area are crucial for multimodal semantic processing: distortion-corrected fMRI evidence for a double gradient of information convergence in the temporal lobes. J Cogn Neurosci 24:1766–1778
41. du Boisgueheneuc F, Levy R, Volle E, Seassau M, Duffau H, Kinkingnehun S, Samson Y, Zhang S, Dubois B (2006) Functions of the left superior frontal gyrus in humans: a lesion study. Brain 129:3315–3328. doi:https://doi.org/10.1093/brain/awl244
42. Coen SJ, Hobson AR, Aziz Q (2012) Chapter 23—processing of gastrointestinal sensory signals in the brain. In: Johnson LR, Ghishan FK, Kaunitz JD, Merchant JL, Said HM, Wood JD (eds) Physiology of the gastrointestinal tract, 5th edn. Academic Press, Boston, pp 689–702
43. Davidson PSR, Anaki D, Ciaramelli E, Cohn M, Kim ASN, Murphy KJ, Troyer AK, Moscovitch M, Levine B (2008) Does lateral parietal cortex support episodic memory? Evidence from focal lesion patients. Neuropsychologia 46:1743–1755. doi:https://doi.org/10.1016/j.neuropsychologia.2008.01.011
44. Meunier D, Lambiotte R, Fornito A, Ersche KD, Bullmore ET (2009) Hierarchical modularity in human brain functional networks. Front Neuroinform 3:37–37. doi:https://doi.org/10.3389/neuro.11.037.2009
45. Fornito A, Zalesky A, Breakspear M (2015) The connectomics of brain disorders. Nat Rev Neurosci 16:159–172. doi:https://doi.org/10.1038/nrn3901
46. Liang X, Zou Q, He Y, Yang Y (2013) Coupling of functional connectivity and regional cerebral blood flow reveals a physiological basis for network hubs of the human brain. Proc Natl Acad Sci 110:1929–1934. https://doi.org/10.1073/pnas.1214900110
47. Aben HP, Biessels GJ, Weaver NA, Spikman JM, Visser-Meily JMA, de Kort PLM, Reijmer YD (2019) Extent to which network hubs are affected by ischemic stroke predicts cognitive recovery. Stroke 50:2768–2774. https://doi.org/10.1161/strokeaha.119.025637
48. Tononi G, Sporns O, Edelman GM (1999) Measures of degeneracy and redundancy in biological networks. Proc Natl Acad Sci 96:3257–3262. https://doi.org/10.1073/pnas.96.6.3257